RESULTS FROM RUN I OF THE TEVATRON

John M. Butler*
Department of Physics
Boston University, Boston MA 02215

Representing the DØ and CDF Collaborations

ABSTRACT

Run I of the Tevatron ended in 1996 but the flow of new physics results based on that data from the CDF and DØ collaborations continues unabated. The Run I physics program is rich and varied, topics include top-quark physics, bottom-quark physics, electroweak studies, QCD studies, and searches for new phenomena. While new results have appeared recently in all areas, this talk will concentrate on those areas that account for the majority of new results: QCD and searches for new phenomena.

*Supported in part by DOE grant DE-FG02-91ER40676.

1 Introduction

The Fermilab Tevatron accelerator collides protons and anti-protons at a center of mass energy of 1.8 TeV. The Tevatron is currently the world's highest-energy accelerator and will continue to be so until the LHC turns on at CERN in ~ 2007. The opportunities for discovery at the energy frontier are well known. The highest-energy collisions allow the resolution of the smallest distance scales as well as allow the creation of new heavy states and particles. The discovery of the top quark at the Tevatron is a prime example of the latter.

The running period from 1992-1996, while not the technically first run of the Tevatron collider, is nonetheless defined as "Run I". Run I *was* the first run featuring both large detectors, CDF and DØ, in data taking. While the bulk of the luminosity was collected at $\sqrt{s} = 1.8$ TeV, there was a short period of running at $\sqrt{s} = 630$ GeV. The 630 GeV data allowed the experiments to explore the energy dependence of various processes as well as to compare with results obtained earlier by the UA1 and UA2 experiments at CERN. CDF and DØ each recorded an integrated luminosity of $\int \mathcal{L}\, dt \sim 0.1$ fb^{-1} during Run I. The time evolution of Run I integrated luminosity is shown in Fig. 1 for DØ.

The CDF[1] and DØ[2] detectors are large general-purpose hadron-collider detectors, see Figs. 2 and 3. Both have inner trackers, calorimetry, and muon systems. The strengths of the two detectors are complimentary. CDF features excellent tracking and charged particle momentum resolution. CDF also had a silicon vertex detector in Run I which allows efficient tagging of b-quark decays. DØ features a highly-segmented and hermetic calorimeter that has superb missing E_T resolution as well as a muon system with very good geometric acceptance.

The Run I physics program is rich and varied. Topics include top-quark physics, bottom-quark physics, electroweak studies, QCD studies, and searches for new phenomena. While there are interesting new results on all fronts, in a brief review of the program such as this choices have to be made to limit the scope of material presented. The majority of results that have come out within the last year are in the areas of QCD and searches for new phenomena, therefore I have chosen to concentrate in these areas. I apologize to the proponents of the many fine analyses that were left out, the choice was pedagogical and not a value judgment on the other work. A complete collection of CDF and DØ papers are available from Refs. 3 and 4. For results listed in the following as "preliminary," refer again to Refs. 3 and 4 for additional details and updates.

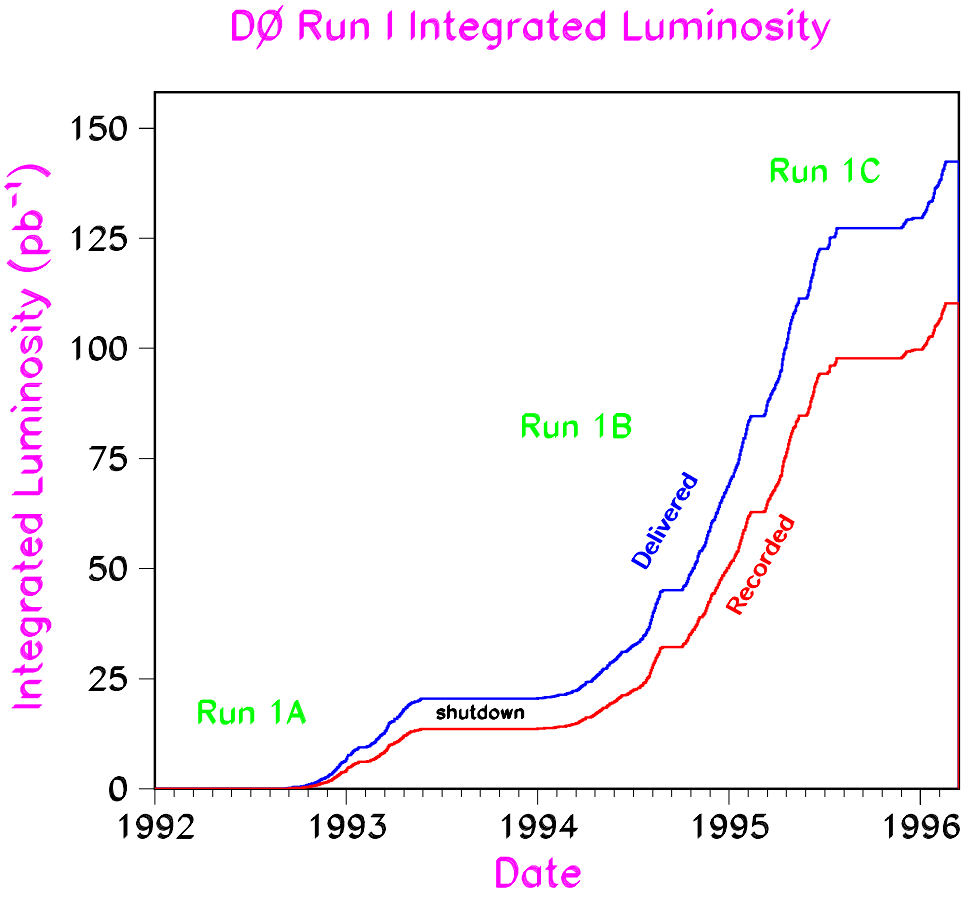

Fig. 1. Accumulation of integrated luminosity as a function of time during Run I for DØ. The distinct running periods Run Ia, Run Ib, and Run Ic are indicated. The $\sqrt{s} = 630$ GeV running occurred during Run Ic.

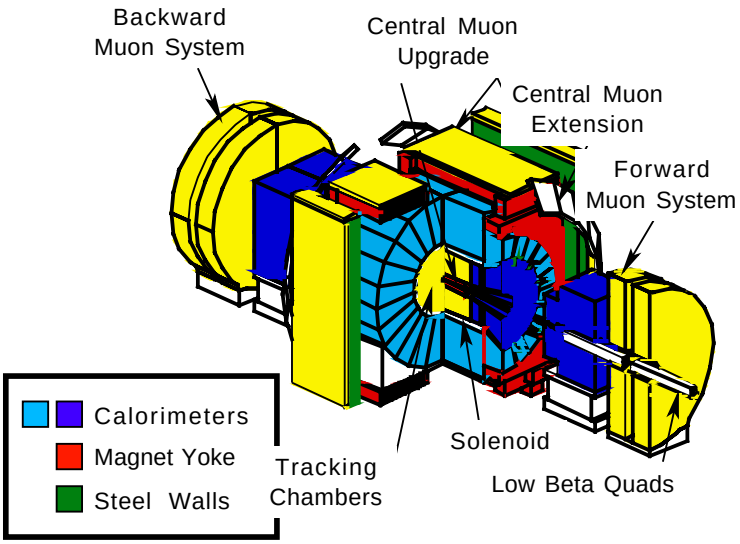

Fig. 2. The Run I CDF detector.

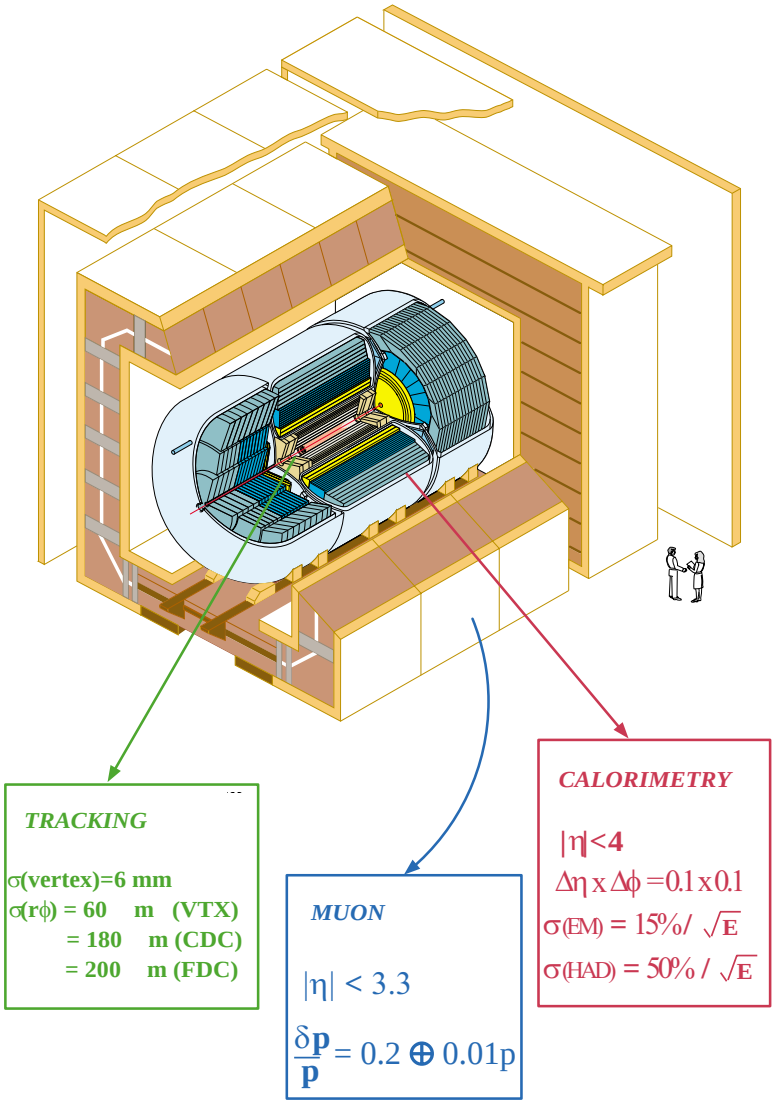

Fig. 3. The Run I DØ detector.

Run I has been extremely productive. There have been about 300 publications from CDF and DØ using Run I data with about 300 students receiving their PhD from Run I analyses. A measure of the vitality of the program is that even now, five years after the end of the run, the rate of publication is not decreasing. This poses a bit of a problem in getting the collaborations to focus fully on the commissioning efforts for Run II but it's the sort of problem one doesn't really mind having! In addition to papers on new physics topics, the latest results contain a mix of detailed documentation of analyses through PRD articles, presentation of innovative analysis techniques, and development of analyses for Run II. The latter may not have great statistical power using Run I data but anticipate the order-of-magnitude increase in data that will come from the ongoing Run IIa.

2 Studying Strong Interactions at the Tevatron

The study of the the strong interaction represents a large portion of the physics program at the Tevatron. About a dozen new papers from CDF and DØ documenting recent QCD results have appeared in the last year. All aspects of the interaction are studied: from the initial partonic luminosities, through the hard scatter, to the final-state hadronization. Many measurements are sensitive to the structure of the proton and anti-proton and provide discriminating power among various parton distribution functions (PDFs). In the hard scatter of quarks and gluons, the renormalization scale and $\sqrt{s}$ dependence of NLO QCD have been investigated. As the partons emerge from the interaction and hadronize, the structure and algorithmic definition of the resulting jets has been studied. A small selection of the new results will be presented here.

2.1 Inclusive Jets

The inclusive jet cross section is one of the flagship measurements at the Tevatron. It provides an incisive test of perturbative QCD and the PDFs. The highest transverse energy jets have $E_T = E \sin\theta \approx 450$ GeV and thus probe distance scales of order 10^{-17}cm. This resolution allows stringent limits to be placed on new physics, for example, quark compositeness. With the latest results from Run I, the inclusive jet cross section measurement enters a new era where the statistical precision has become much better than the uncertainty in the experimental systematics and theoretical predictions.

The new result from CDF for inclusive jets in Run Ib is based on $\int \mathcal{L}\, dt = 87$ pb^{-1}

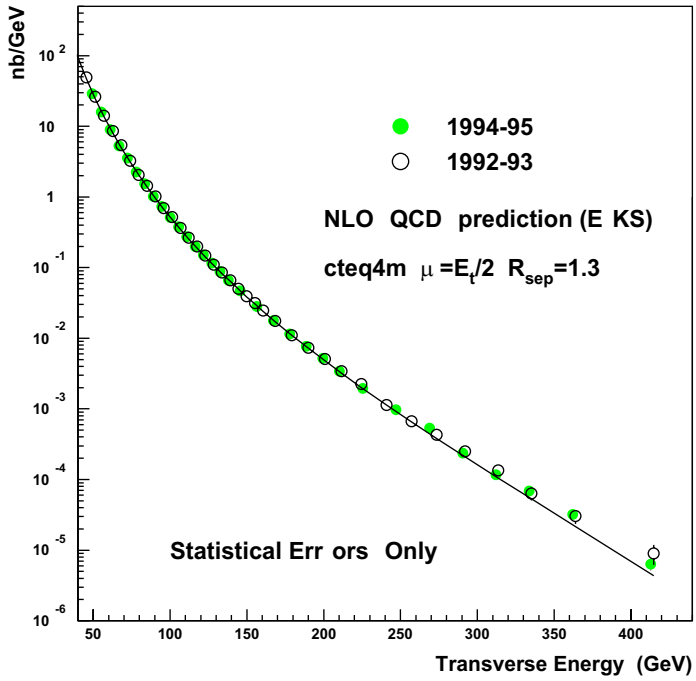

Fig. 4. The inclusive jet cross section vs. E_T from CDF is shown along with the NLO QCD prediction.

(Ref. 5). The geometric acceptance in pseudo-rapidity η, where $\tanh \eta = \cos \theta$, is in the central region, $0.1 < |\eta| < 0.7$. The cross section as a function of E_T is shown in Fig. 4. Good agreement between the data and the NLO QCD prediction is seen over seven orders of magnitude. To observe discrepancies between data and theory more easily, it is customary for these measurements to plot the ratio of (Data – Theory)/Theory. This ratio is shown in Fig. 5 versus E_T for three current PDFs. Again, generally good agreement with NLO QCD is observed although the data favors the CTEQ4HJ PDF. This is not surprising, however, because CTEQ4HJ has already incorporated earlier Tevatron high E_T jet data into the fit. The consequence is that CTEQ4HJ has a higher gluon content at high x and thus better describes the high E_T end of the spectrum.

The new result from DØ for inclusive jets in Run Ib is based on $\int \mathcal{L}\, dt = 95$ pb^{-1} (Ref. 6). DØ extends the geometric acceptance into the forward region by requiring jets with $|\eta| < 3.0$, this significantly enhances the kinematic reach. Fig. 6 shows how the DØ measurement covers previously unexplored regions in x at high Q^2. Fig. 7 shows the DØ inclusive jet cross section as a function of E_T for five different bins

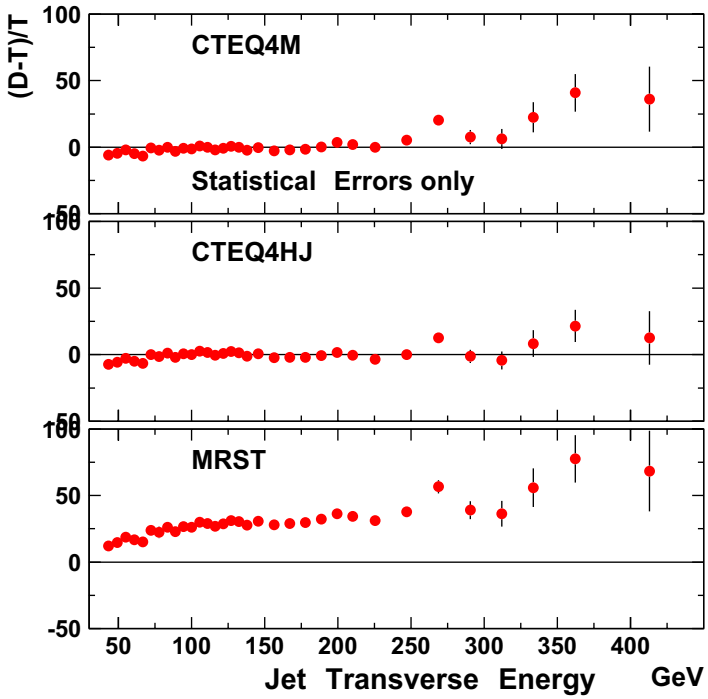

Fig. 5. Comparison of CDF inclusive jet data to theoretical predictions using the CTEQ4M, CTEQ4HJ, and MRST PDFs.

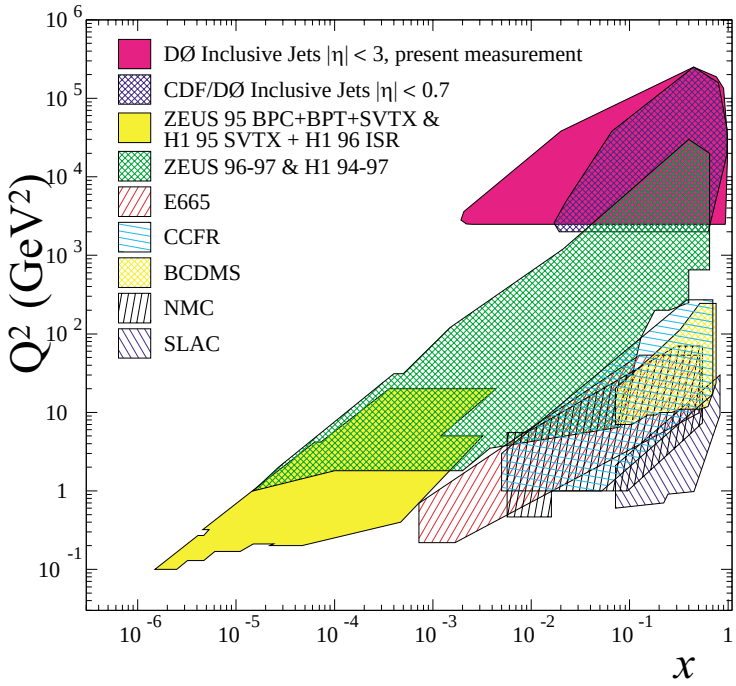

Fig. 6. The kinematic reach of DØ inclusive jets data compared to other experiments.

in $|\eta|$. Good agreement is observed between the data and the NLO QCD prediction for all geometric regions. This is seen more clearly in the (Data – Theory)/Theory plots in Fig. 8 where the error bars indicate statistical uncertainties and the bands show the systematic uncertainty. The conclusion drawn by DØ is that the data prefer the CTEQ4HJ, MRSTg↑, and CTEQ4M PDFs.

2.2 Dijet Triple Differential Cross Section at CDF

The large data sets from Run I allow a more detailed analysis of the jet data which could reveal subtle effects that might otherwise be lost in integrating over kinematic variables. A good example is the preliminary dijet triple differential cross section measured by CDF. The analysis goes beyond the inclusive jet cross section by examining the properties of the two leading jets. This result is based on $\int \mathcal{L}\, dt = 86$ pb^{-1} collected at $\sqrt{s} = 1800$ GeV. CDF measures the 2-jet differential cross section $d^3\sigma/dE_T d\eta_1 d\eta_2$ as a function of the E_T of the leading jet, called jet 1. Jet 1 is required to be central, $0.1 < |\eta_1| < 0.7$, while jet 2 is restricted to four bins within $0.1 < |\eta_2| < 3.0$. Fig. 9 shows the preliminary CDF result where the data is compared to NLO QCD for a num-

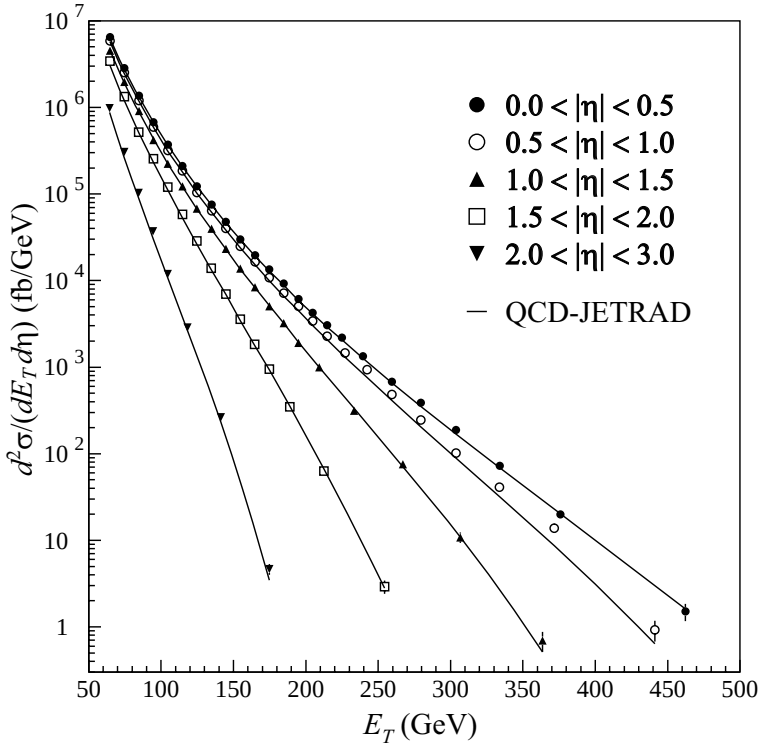

Fig. 7. The inclusive jet cross section vs. E_T from DØ for five $|\eta|$ bins is shown along with the NLO QCD prediction.

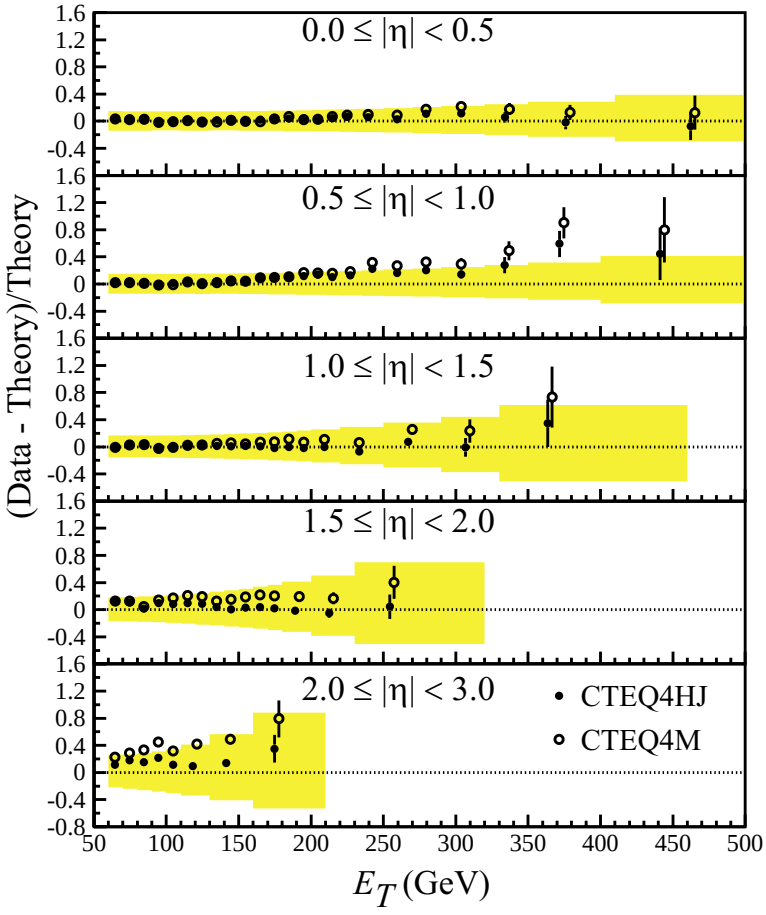

Fig. 8. Comparison, in five $|\eta|$ bins, of DØ inclusive jet data to theoretical predictions using the CTEQ4HJ and CTEQ4M PDFs.

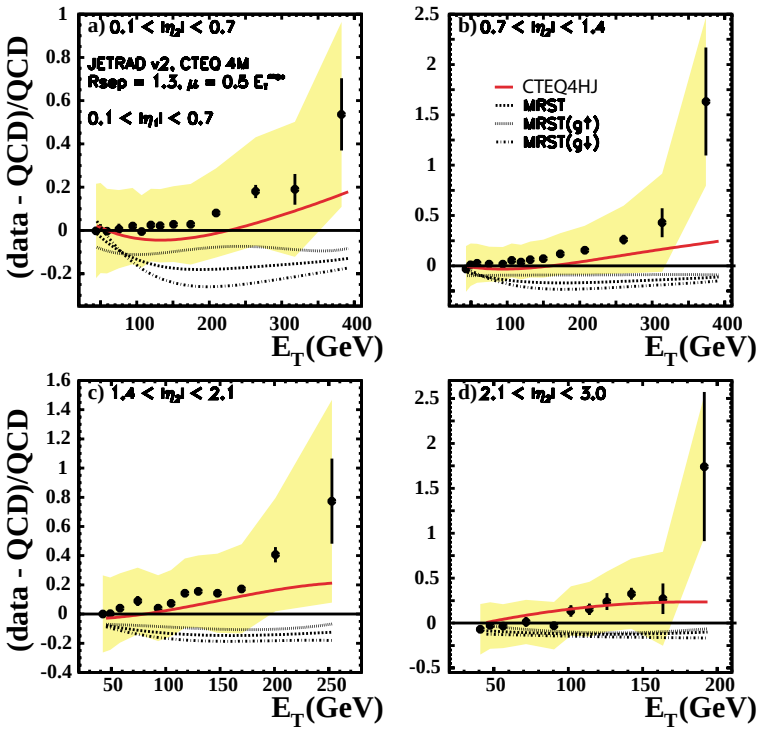

Fig. 9. The preliminary dijet triple differential cross section from CDF in four $|\eta|$ bins of acceptance for the second leading jet.

ber of different PDFs. In the inclusive jet cross section measurement, CDF found good agreement with the CTEQ4HJ PDF while in this analysis the conclusion is that *none* of the PDFs examined provides a good description of the data.

2.3 Direct Photons at the Tevatron

The primary production mechanism for direct photons at the Tevatron is gluon Compton scattering $qg \to \gamma q$. Direct photons are thus sensitive to the gluon distribution in the proton. They provide a very clean probe compared to quarks and gluons which have the fragmentation and algorithmic problems associated with jets in the final state. The status of direct photon cross section measurements is that earlier experiments consistently reported an excess at low photon E_T. This excess was attributed to some combination of limitations in the NLO QCD predictions and shortcomings in the available PDFs. The new measurements from CDF and DØ seek to address this issue.

DØ has measured the direct photon cross section at $\sqrt{s} = 630$ using $\int \mathcal{L}\, dt = 520$ nb^{-1} (Ref. 7). Fig. 10 shows the comparison (Data – Theory)/Theory as a function

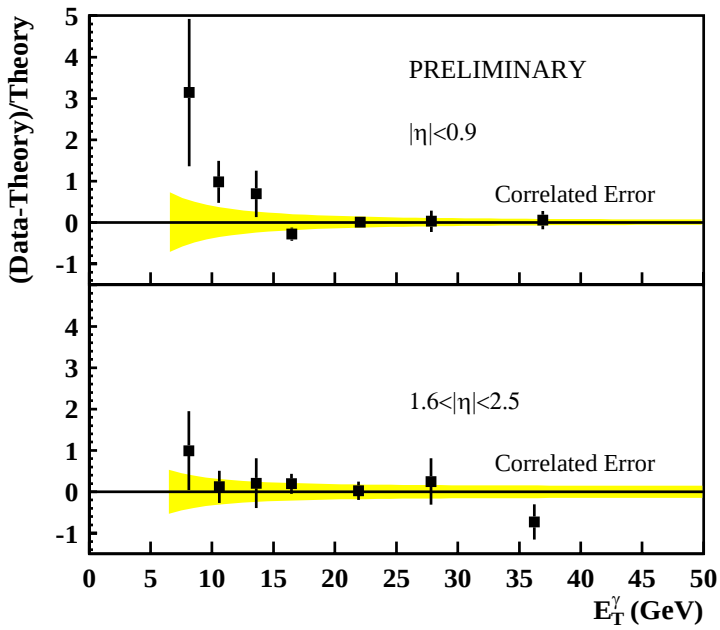

Fig. 10. The direct photon cross section from DØ at $\sqrt{s} = 630$ GeV compared to the NLO QCD prediction. The shaded bands indicate the correlated uncertainty.

of photon E_T for photons in the central, $|\eta| < 0.9$, and forward, $1.6 < |\eta| < 2.5$, regions. The data agrees with the QCD prediction (the fit probability is 12% (71%) for the central (forward) region) although an excess at low E_T is observed.

DØ also uses this data to measure the dimensionless cross section

$$\sigma_D = \frac{E_T^3}{2\pi} \frac{d^2\sigma}{dE_T d\eta}$$

as a function of $x_T = 2E_T/\sqrt{s}$. Naïvely, σ_D does not depend on $\sqrt{s}$ and so the ratio of σ_D measured at different $\sqrt{s}$ is unity. A more sophisticated treatment of the cross section ratio modifies the naïve prediction somewhat. Because many systematic uncertainties cancel in the ratio $\sigma_D(\sqrt{s} = 630)/\sigma_D(\sqrt{s} = 1800)$, it provides a good test of QCD. Fig. 11 shows this ratio, binned in central and forward regions as before. Good agreement between the ratio and theory is observed.

CDF has preliminary results on direct photon cross sections at $\sqrt{s} = 1800$ and 630 GeV. The old Run Ia and new Run Ib results at 1800 GeV are consistent with each other but the Run Ib result has considerably higher statistical power. CDF observes

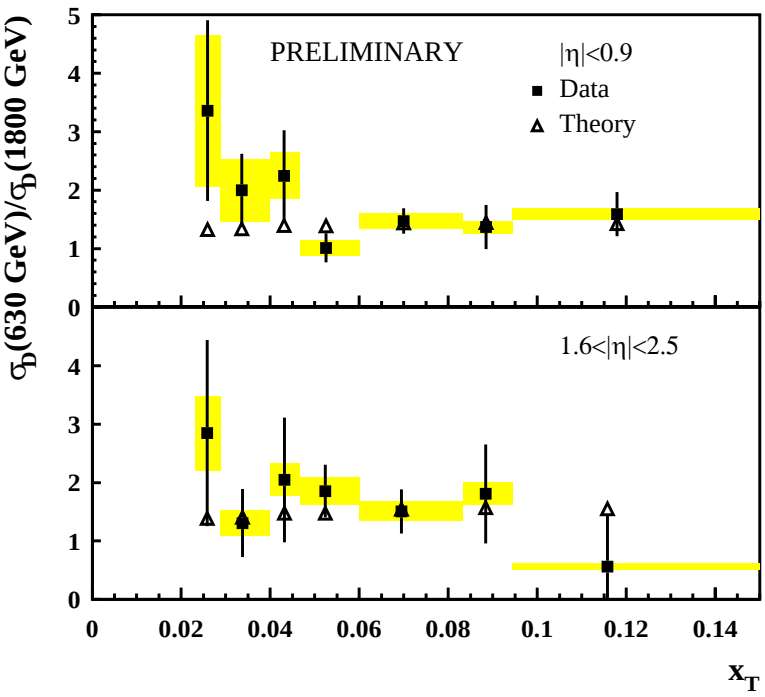

Fig. 11. The ratio of direct photon cross sections at $\sqrt{s} = 630$ GeV to $\sqrt{s} = 1800$ GeV from DØ compared to the NLO QCD prediction. The shaded bands indicate the correlated uncertainty.

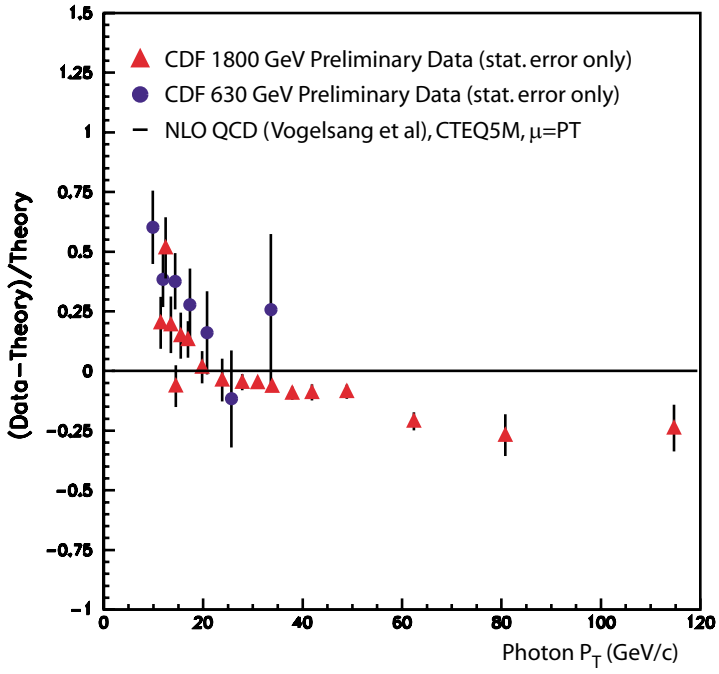

Fig. 12. Comparison of theory to preliminary direct photon cross sections measured at $\sqrt{s} = 630$ and 1800 GeV by CDF as a function of photon P_T.

significant systematic differences in shape between data and theory. Fig. 12 plots (Data – Theory)/Theory as a function of photon P_T for the Run Ib and 630 GeV results. The cross sections at the two energies are consistent with each other but do not follow the NLO QCD prediction. In addition, a large discrepancy is seen between the Run Ib and 630 GeV data when plotted as a function of photon $x_T = 2P_T/\sqrt{s}$, see Fig. 13. More work will be needed to understand these discrepancies, it appears there are still a few surprises to be found in studies of QCD!

3 Searches for New Phenomena

It is well known that the Standard Model (SM) of particle physics provides an excellent description of nature. Currently, there is no experimental result that is in significant disagreement with the SM. And yet, despite the overwhelming success of the SM, it is rather ironic that essentially nobody in HEP believes the SM is the complete picture of particle physics. As a result, many extensions and alternative to the SM have been

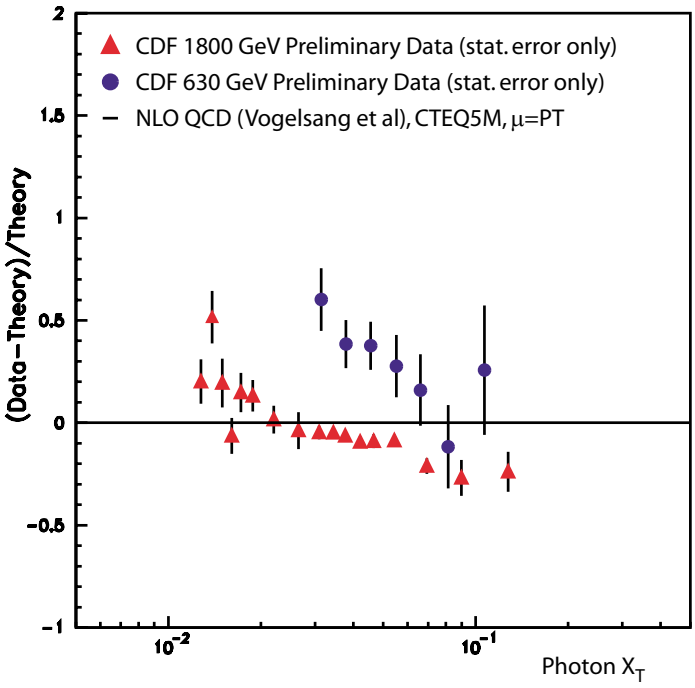

Fig. 13. Comparison of theory to preliminary direct photon cross sections measured at $\sqrt{s} = 630$ and 1800 GeV by CDF as a function of photon $x_T = 2P_T/\sqrt{s}$.

proposed. In looking for new physics beyond the SM, there are distinct advantages to searching at the highest available energies. With its position at the energy frontier, the Tevatron is a sensitive probe of new phenomena.

Many new theoretical models and ideas have emerged since the end of Run I, a good example being large extra dimensions. Therefore, the exotics groups at CDF and DØ continue to remain very active with a wide range of new searches for physics beyond the SM appearing in the last year. Topics include searches for SUSY gluinos and squarks, R parity violating (RPV) SUSY, technihadrons from new strong dynamics, new heavy gauge bosons, leptoquarks, quark-lepton compositeness, large extra dimensions (LED), charged Higgs bosons, and more. A small selection of the new results will be presented here.

3.1 Search for Scalar Top Quarks at DØ

This analysis[8] considers SUSY models where the scalar top (stop) is the lightest squark. In the MSSM where the LSP is the sneutrino, the stop decay $\tilde{t} \rightarrow b\ \tilde{\chi}_1^+ \rightarrow b\ \ell\ \tilde{\nu}$ is dominant. Therefore, the final state at the Tevatron generally contains two charged leptons, 2 b-quarks, and missing energy: $p\bar{p} \rightarrow 2\ell\ 2b\not\!\!E_T$. This analysis restricts itself to the $p\bar{p} \rightarrow e\mu\not\!\!E_T$ channel. The main backgrounds to contend with are (1) instrumental: multi-jet events with a jet faking an electron plus fluctuations causing apparent $\not\!\!E_T$, and (2) physics processes with the same final state as the signal: $Z \rightarrow \tau^+\tau^-$, $WW \rightarrow e\mu\nu\nu$, $t\bar{t} \rightarrow e\mu\nu\bar{\nu}jj$, and Drell-Yan $\rightarrow \tau^+\tau^-$. The event selection is essentially the same as for the published DØ top-quark cross-section analysis in the same final state. Using $\int \mathcal{L}\ dt = 108$ pb^{-1}, DØ observes 10 candidate events where 13.7 events are expected from the SM and 13.2 events for a stop mass of 120 GeV. In the absence of a stop signal, DØ places limits in the stop-sneutrino mass plane, see Fig. 14. This analysis significantly enlarges the exclusion region beyond earlier results, excluding a stop with mass up to 144 (130) GeV for a sneutrino mass of 45 (85) GeV.

3.2 Search for RPV Stop at CDF

In SUSY there is a new quantum number "R parity." It is defined as $R_P \equiv (-1)^{3B+L+2S}$, $R_P = +1$ for particles and $R_P = -1$ for sparticles. If R_P is conserved, sparticles are pair-produced and the LSP is stable. This scenario leads to the classic large-missing-E_T signature that has been used in many previous SUSY searches. In the case of R_P-violation (RPV), new signatures become important. The model considered here

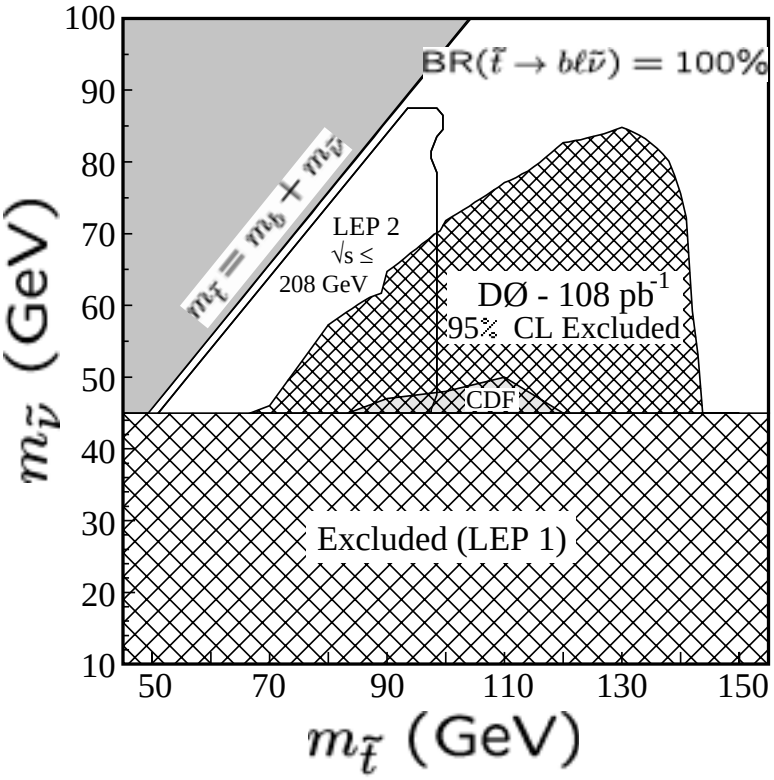

Fig. 14. The 95% CL exclusion regions in the stop-sneutrino mass plane from the DØ, CDF, and LEP experiments.

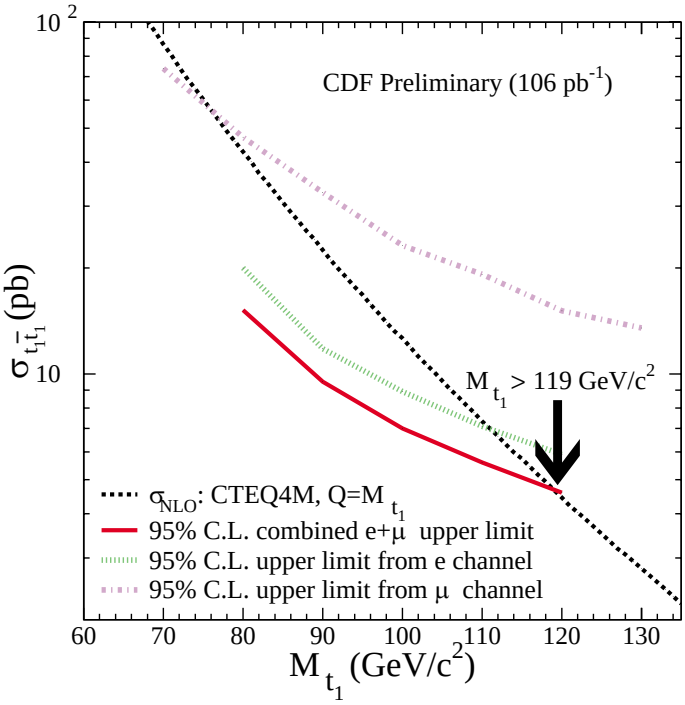

Fig. 15. The cross section for RPV stop as a function of stop mass is shown along with preliminary 95% CL upper limits from CDF in the e, μ, and combined $e\mu$ channels.

assumes there is RPV in the third generation and the LSP is the stop, thus the decay $\tilde{t}_1 \to \tau^+ b$ dominates. CDF searches for this signal by looking for two tau leptons in the final state with one τ decaying leptonically and the other hadronically (τ_h). The final state contains the decay chain $\tilde{t}_1\bar{\tilde{t}}_1 \to \tau^+ b \tau^- \bar{b} \to \ell\ \tau_h\ 2j\ X$ where $\ell = e, \mu$ and the BR$(\tilde{t}_1 \to \tau^+ b) = 100\%$ is assumed. Identifying tau leptons at a hadron collider is not easy but CDF has demonstrated their τ ID efficacy by observing $Z \to \tau\tau$ in this mode. Using $\int \mathcal{L}\, dt = 106$ pb^{-1}, CDF observes no candidate events after all selection criteria have been applied. In the absence of a signal, CDF sets a preliminary 95% CL lower limit on the stop mass of 119 GeV, see Fig. 15.

3.3 Search for Quark-Lepton Compositeness and W' at CDF

The two results described in this subsection both make use of the $e\nu$ final state. The transverse mass $m_T(e\nu)$ distribution, shown in Fig. 16 for $\int \mathcal{L}\, dt = 106$ pb^{-1}, is dominated by the W boson. This work analyzes the shape of the $m_T(e\nu)$ distribution for large $m_T(e\nu)$ because the high $m_T(e\nu)$ tail can be used to probe for extensions to the

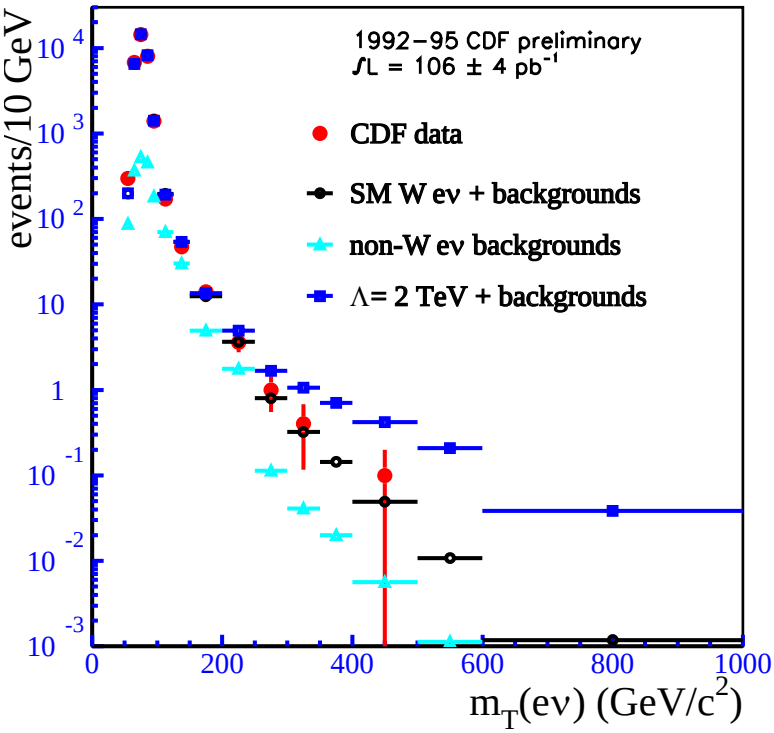

Fig. 16. The preliminary $e\mu$ transverse mass $m_T(e\nu)$ distribution from CDF. Also shown are the estimates of the backgrounds and the effect of quark-lepton compositeness with scale $\Lambda = 2$ TeV.

SM. Here two classes of models are considered:

1. Models where SM fermions are composite, bound by new strong dynamics. Experimentally, this appears as a 4-fermion contact interaction with characteristic scale Λ.
2. Models with larger gauge groups that predict new gauge bosons W' and Z'.

In both cases, the new physics gives an enhancement at high $m_T(e\nu)$ compared to the SM. The SM prediction from Monte Carlo is normalized to the inclusive W data.

As seen in Fig. 16, at high $m_T(e\nu)$ the background prediction is dominated by real W events and other backgrounds are small. The good agreement of data with the SM prediction allows CDF to exclude, at the 95% CL, quark-lepton compositeness with scale $\Lambda < 2.81$ TeV and W' masses below 786 GeV. Both results are preliminary.

3.4 Search for Technihadrons at DØ

Much as CDF used the $e\nu$ final state in the last section, DØ uses the ee final state to search for new physics.[9] The DØ dielectron mass distribution, based on $\int \mathcal{L}\, dt = 125$ pb^{-1}, is shown in Fig. 17. The distribution is dominated by the Z boson.

While a number of models of new physics predict an enhancement at large dielectron mass, this analysis concentrates on the search for particles resulting from topcolor-assisted technicolor. In this model, the production of the lightest technihadrons $\pi_T,\ \rho_T,\ \omega_T$ has substantial rate at the Tevatron. The corresponding decay channels are $\rho_T, \omega_T \to \gamma\pi_T,\ W\pi_T$, and $f\bar{f}$. This work analyzes the dielectron channel $p\bar{p} \to \rho_T, \omega_T \to e^+e^-$ and assumes $M_{\rho_T} = M_{\omega_T}$. As seen in Fig. 17, good agreement is observed between the data and the SM background prediction. In the absence of a significant excess above background, DØ proceeds to set limits on technihadron masses. The precise cross section and branching fraction predictions depend on a number of details of the model, such as the technihadron masses and a mass parameter M_T. Nonetheless the resulting limits end up being somewhat insensitive to these details: DØ sets 95% CL limits of $M_{\rho_T,\omega_T} > 207$ GeV if $M_{\rho_T} - M_{\pi_T} < M_W$ and $M_{\rho_T,\omega_T} > 203$ GeV if $M_T > 200$ GeV.

3.5 Search for Large Extra Dimensions at the Tevatron

There has been much recent interest in the possibility that our world has a number of extra spatial dimensions that may be "large." Theories with large extra dimensions (LED) have the attractive feature that they solve the hierarchy problem by effectively lowering the Planck scale to the electroweak scale.

The size R of the extra dimensions depends on the number n extra dimensions in the theory as

$$R \sim \frac{1}{M_S}\left(\frac{M_{Pl}}{M_S}\right)^{2/n}$$

where M_S is the effective Planck scale. Until recently, extra dimensions as large as $\mathcal{O}(1\ \mathrm{mm})$ were not excluded experimentally. New results from Cavendish-style torsion-balance experiments and cosmological constraints likely rule out $n = 2$. For $n > 2$, the extra dimensions become microscopic and a new measurement technique is needed. Experiments at the LEP and Tevatron colliders are sensitive to LED for $n > 2$ and can push the limits further. Graviton emission and exchange involving SM particles is greatly enhanced in LED theories. At the Tevatron, this leads to three ba-

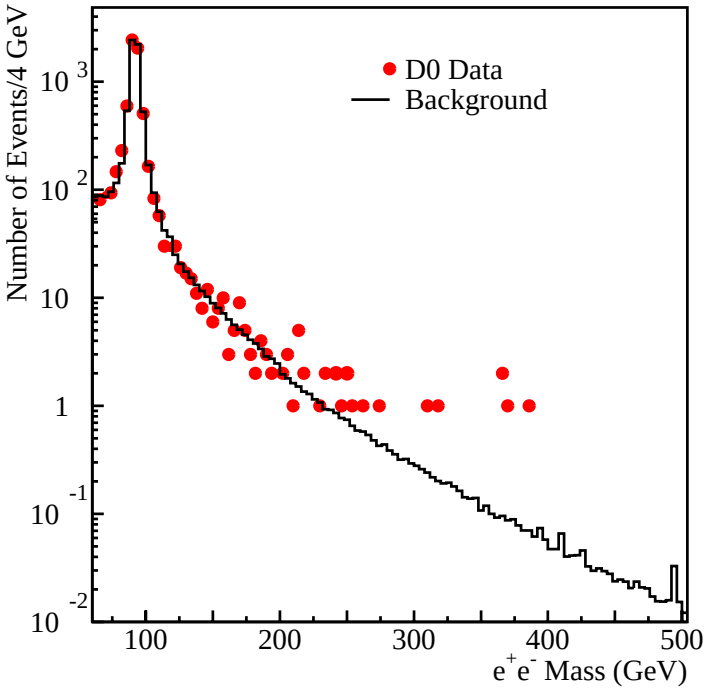

Fig. 17. The dielectron mass distribution from DØ, where the data are plotted as dots and the SM background prediction is the histogram.

Giudice, Rattazzi, Wells[11]	Han, Lykken, Zhang[12]		Hewett[13]
	$n = 2$	$n = 7$	$\Lambda = +1(-1)$
1.2 TeV	1.4 TeV	1.0 TeV	1.1 (1.0) TeV

Table 1. DØ 95% CL limits on the effective Planck scale M_S for three models of LED.

sic signatures: (1) graviton emission in normal jet production, in particular, an excess of "monojet" events, (2) graviton emission in conjunction with vector bosons, and (3) effects from virtual graviton exchange in the s-channel. The most promising of these signatures is virtual graviton exchange and this has been the channel used by CDF and DØ in searches to date.

DØ searches for virtual graviton effects in the dielectron and diphoton final states $p\bar{p} \to e^+e^-X$ or $\gamma\gamma X$ (Ref. 10). To maximize the overall efficiency, the requirement of having a track is relaxed in defining the electron. In effect, DØ observes "di-EM" final states. The background in the high M_{EM-EM} region of interest is from real γ-γ events, so tight ID is not required. The signal for LED shows up as an excess of events at high M_{EM-EM} and low $|\cos\theta^*|$, see Fig. 18. In the absence of a LED signal, DØ places lower limits on the effective Planck scale for several current models, see Table 1. These limits are similar to those obtained by experiments at LEP.

CDF has made a preliminary search for LED in the dielectron final state $p\bar{p} \to e^+e^-X$. The event selection is based on their published Z' search. After requiring events with two central energetic electrons, the dielectron mass is plotted, see Fig. 19. The SM expectation is normalized in the Z region. Models of LED predict an excess at high dielectron mass. With no excess above SM background observed, CDF places preliminary limits on the effective Planck scale M_S in the context of the Hewett model:

- $M_S > 0.855$ TeV for $\Lambda = +1$
- $M_S > 0.840$ TeV for $\Lambda = -1$

CDF will improve these results by extending the geometric coverage of the electrons used in the analysis and by including the diphoton final state.

3.6 QUAERO: a General Interface to DØ Event Data

As the previous sections may have made clear, it is often the case that many different models of new physics are tested against a given final-state data set. Rather than have the Tevatron experimenters check every new model that comes along and set limits

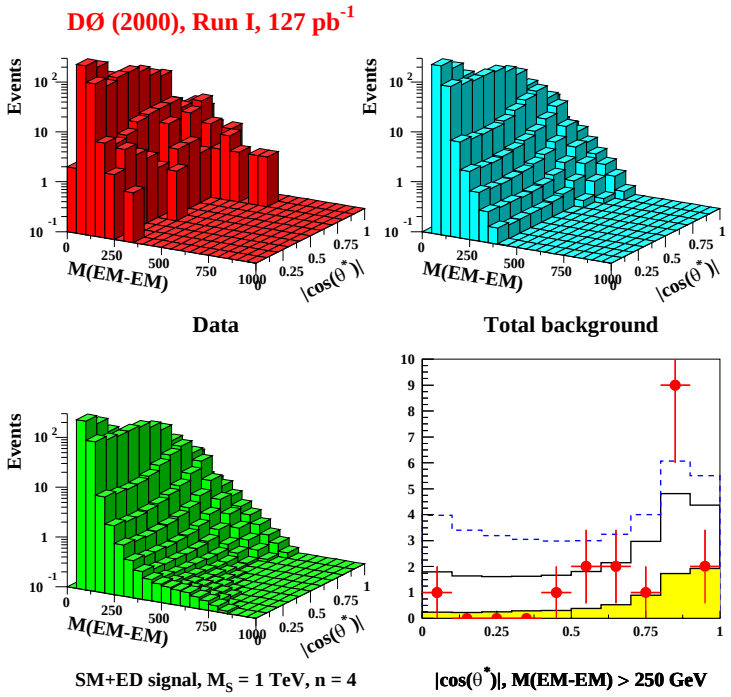

Fig. 18. Two-dimensional distributions from DØ in di-EM mass and $|\cos\theta^*|$ for: (upper left) data, (upper right) background, (lower left) background and LED signal for $M_S = 1$ TeV and $n = 4$, and (lower right) $|\cos\theta^*|$ distribution for events with $M_{EM-EM} > 250$ GeV, where the filled circles correspond to the data, instrumental background is shown shaded, the entire background from SM sources is given by the solid line, and the dotted line corresponds to the sum of SM and LED for the model parameters considered.

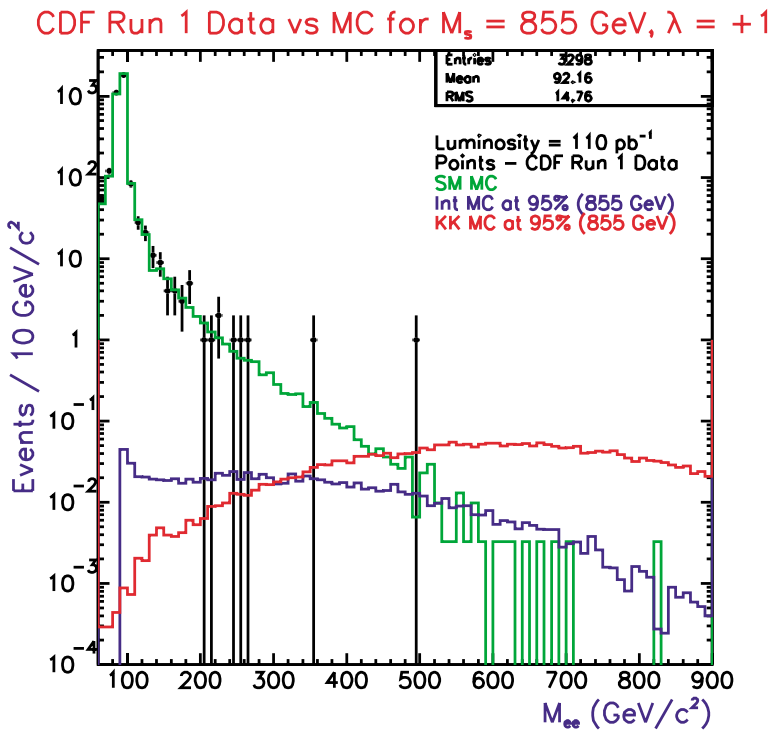

Fig. 19. The dielectron mass distribution from CDF is shown as data points along with the SM background estimate and two contributions from LED — virtual graviton exchange and SM-LED interference. The LED prediction is from the Hewett model with $M_S = 855$ GeV and $\Lambda = +1$, the signal would appear as an excess at high M_{ee}.

with their own data, the purpose of QUAERO[14] is to allow anyone with a new model to check it themselves. QUAERO is a tool to make HEP data (in this case, DØ Run I data) publicly available. At present, the inclusive final states that are available for use in QUAERO are $e\mu$, $e\not{E}_T\ 2j$, and $ee\ 2j$. By "inclusive" it is meant that the final state may include additional jets. If a user has a model to test against one or more of these final states, then they specify the signal and relevant variables to QUAERO through a web interface.[15] QUAERO first automatically calculates the optimized signal vs. background selected region in the parameter space defined by the supplied variables, then compares to DØ data, and finally returns $\sigma^{95\%}$, the 95% CL upper limit cross section, to the user. QUAERO has been tested on many processes and has performed consistently well, two examples are given here. Fig. 20 (top) shows the signal and background probability densities returned by QUAERO when it is asked to look for top-quark production in the $e\mu$ final state. The shaded selected region in the Σp_T^j (scalar sum of jet E_T's) vs. p_T^e plane shows two events are found. The slight excess over background is consistent with the known top-quark $\sigma\cdot$BR. Fig. 20 (bottom) shows similar plots for a search for 225 GeV leptoquarks in the $ee\ 2j$ final state. In this test case, QUAERO reproduces the published DØ leptoquark limit in this channel. New users of QUAERO are encouraged and welcome.

4 Summary

Analysis of the data from Run I of the Tevatron continues to be very active. CDF and DØ are still producing world class results from the many ongoing analyses covering a wide range of physics topics. Although the pace of Run I publications has not slackened, the emphasis of the collaborations is now shifting to Run II commissioning and data taking. There is considerable reason for excitement about the prospects for Run II physics:

- Higher $\sqrt{s}$, from 1.8 TeV to 2.0 TeV, means a 30-40% higher production cross section for "heavy" particles like top quarks.
- Upgraded detectors with greatly improved capabilities.
- Large data sets – the current Fermilab plan is to collect $\mathcal{L} = 15$ fb^{-1} for Run IIb.

Given all this, there will clearly be a multitude of new results from the Tevatron to report at the SLAC Summer Institute for many years to come.

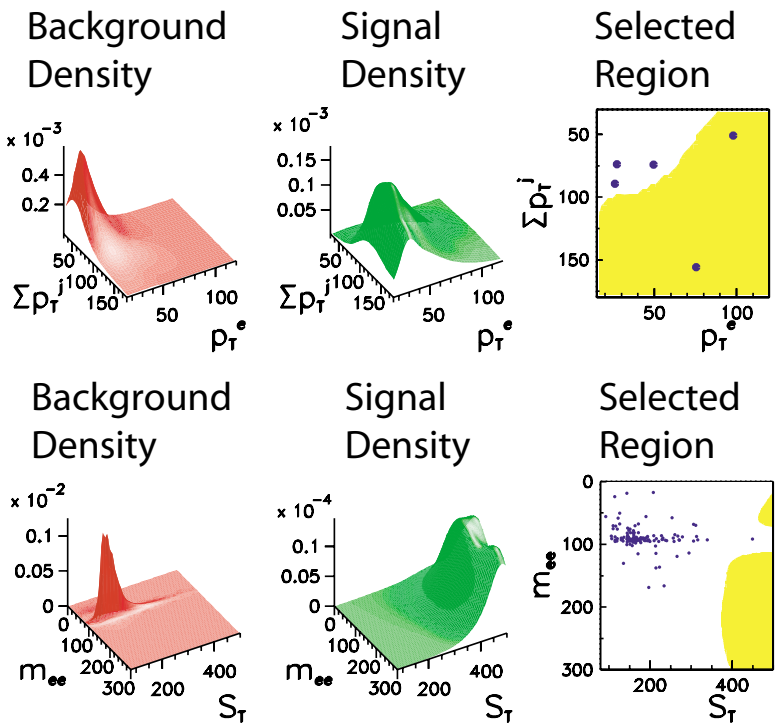

Fig. 20. The (left column) background density, (center column) signal density, and (right column) selected (shaded) region determined by QUAERO for two potential signals: (top row) $t\bar{t} \to e\ \mu \not{E}_T\ 2j$ and (bottom row) $LQ_{225}\overline{LQ}_{225} \to e\ e\ 2j$. The dots in the selected region plots represent events observed in the data.

5 Acknowledgments

I attended my first Summer Institute in the early 1980's while a student at Stanford and it is always a pleasure to return to SLAC. I want to express my gratitude to the meeting organizers for their generous invitation and hospitality. I also want to thank my friends and colleagues from the DØ and CDF collaborations who helped with the preparation of this talk.

References

[1] CDF collaboration (F. Abe et al.), Nucl. Instr. & Meth. **A271**, 387 (1988).

[2] DØ collaboration (S. Abachi et al.), Nucl. Instr. & Meth. **A338**, 185 (1994).

[3] `http://www-cdf.fnal.gov/`.

[4] `http://www-d0.fnal.gov/`.

[5] CDF collaboration (T. Affolder et al.), FERMILAB-PUB-01/008/E, accepted for publication by Phys. Rev. D.

[6] DØ collaboration (B. Abbott et al.), Phys. Rev. Lett. **86**, 1707 (2001).

[7] DØ collaboration (V.M. Abazov et al.), hep-ex/0106026 (2001).

[8] DØ collaboration (V.M. Abazov et al.), hep-ex/0108018 (2001).

[9] DØ collaboration (V.M. Abazov et al.), Phys. Rev. Lett. **87**, 61802 (2001).

[10] DØ collaboration (B. Abbott et al.), Phys. Rev. Lett. **86**, 1156 (2001).

[11] G. Giudice, R. Rattazzi, and J. Wells, Nucl. Phys. **B544**, 3 (1999).

[12] T. Han, J.D. Lykken, and R.-J. Zhang, Phys. Rev. D **59**, 105006 (1999).

[13] J.L. Hewett, Phys. Rev. Lett. **82**, 4765 (1999).

[14] DØ collaboration (V.M. Abazov et al.), hep-ex/0106039 (2001).

[15] `http://quaero.fnal.gov/quaero`.